Modelling of Concrete Behaviour with a Non-Local Continuum Damage Approach

Jerzy Bobiński, Jacek Tejchman

Gdańsk University of Technology Faculty of Civil and Environmental Engineering
80-952 Gdańsk, ul. Narutowicza 11/12, Poland, e-mails: bobin@pg.gda.pl, tejchmk@pg.gda.pl

Abstract

The paper presents FE-results on the behaviour of concrete under plane strain conditions. The material was modelled using a simple isotropic damage continuum model. The model was enriched by non-local terms to avoid a pathological mesh-sensitivity and to obtain a well-posed rate boundary value problem. The constitutive model was used to simulate localization of deformation in 3 benchmark problems: a double-edge notched specimen under uniaxial tension and a notched beam under three- and four-point bending. Attention was laid on the effect of a characteristic length on the load-displacement curves and strain localization. The FE-results were compared with experiments and other numerical studies.

Key words: characteristic length, concrete, crack, damage model, FEM, non-local theory

1. Introduction

Concrete is a highly heterogeneous, discrete, anisotropic, brittle material with a very complex non-linear mechanical behaviour due to the occurrence of localization of deformation. The localization of deformation can occur as cracks (mode I) if cohesive properties are dominant or shear zones (mode II) if frictional properties prevail. As a result of strain localization, material softening takes place and a significant reduction of the material stiffness during cyclic loading-occurs. An understanding of the mechanism of the formation of localization is of crucial importance since they act as a precursor to ultimate fracture and failure.

To describe the behaviour of quasi-brittle materials, different models have been developed: continuum ones within fracture mechanics (Bazant and Cedolin 1979, Hilleborg 1989), damage mechanics (Dragon and Mróz 1979, di Prisco and Mazars 1996, Chen 1999, Ragueneau et al. 2000), plasticity (Willam and Warnke 1975, de Borst 1986. Pietruszczak et al. 1988, Menetrey and Willam 1995, Lade and Jakobsen 2002, Bobinski and Tejchman 2004), coupled damage and plasticity

(Lemaitre 1985, Klisinski and Mróz 1988, de Borst et al. 1999, Ibrahimbegovic et al. 2003), microplane theory (Bazant and Ozbolt 1990, Jirasek 1999) and discrete ones using a lattice approach (Herrmann et al. 1989, Vervuurt et al. 1994, Bobinski et al. 2005) and DEM (Sakaguchi and Mühlhaus 1997, Donze et al. 1999, Place and Mora 2001).

Classical FE-simulations of the behaviour of materials with strain localization are not able to describe properly both the thickness of localization and distance between them. They suffer from mesh sensitivity (its size and alignment) and produce unreliable results. The strains concentrate in one element wide zones and the computed force-displacement curves are mesh-dependent (especially in a post-peak regime). The reason is that differential equations of motion change their type (from elliptic to hyperbolic in static problems) and the rate boundary value problem becomes ill-posed. Thus, classical constitutive models require an extension in the form of a characteristic length to properly model the thickness of localized zones. Such extension can by done with a micro-polar (Mühlhaus 1986, Sluys 1992, Tejchman and Wu 1993, Tejchman et al. 1999), strain gradient (Zbib and Aifantis 1989, Mühlhaus and Aifantis 1991, Pamin 2004, Sluys and de Borst 1994, Peerlings et al. 1998, Meftah and Reynouard 1998, Pamin and de Borst 1998, Chen et al. 2001, Askes and Sluys 2003), viscous (Neddleman 1988, Loret and Prevost 1990, Sluys 1992, Ehlers and Graf 2003) and non-local terms (Bazant 1986, Pijaudier-Cabot and Bazant 1987, Bazant and Lin 1988, Brinkgreve 1994, de Vree et al. 1995, Strömberg and Ristinmaa 1996, Marcher and Vermeer 2001, Maier 2002, 2003, di Prisco et al. 2002, Bazant and Jirasek 2002, Jirasek and Rolshoven 2003, Tejchman 2004).

Another numerical technique which enables to remedy the drawbacks of standard FE-methods and to obtain mesh-independent results during the description of strain localization is the so-called strong discontinuity approach which affords a finite element with a displacement discontinuity (Regueiro and Borja 2001, Vermeer et al. 2004, Simone and Sluys 2004). However, the approach cannot describe the patterning of strain localization and wall strain localization along structures and does not include a characteristic length to investigate a size effect.

The intention of the paper was to analyze localization of deformations in the form of cracks (mode I) in quasi-brittle materials (e.g. concrete-like materials) during such tension dominated problems as uniaxial tension and bending using an FE-method based on a non-local damage continuum model. Due to the presence of a characteristic length, the law can describe the formation of strain localization (its thickness and spacing). The FE-results converge to a finite size of strain localization via mesh refinement, and the initial and boundary value problem becomes mathematically well-posed at the onset of localization. The presence of a characteristic length also enables the capture of a scale effect (dependence of strength and other mechanical properties on the size of the specimen) observed experimentally on softening granular and

brittle specimens. This is made possible since the ratio l_c/L governs the response of the model (l_c – characteristic length, L – size of the structure) (Tejchman 2004). The advantages of this model is extremely simple, a small amount of material constants and consideration of the stiffness degradation. The drawback is the lack of plastic deformations and hardening. The potential of the model to describe strain localization was demonstrated with the FE-results of three different tension dominated boundary value problems: uniaxial tension, three-point bending and four-point bending. The FE-results were compared with the experimental ones and other FE-solutions. The influence of a characteristic length on the load-displacement curves and the related size effect were studied.

2. Constitutive Model

Continuum damage models initiated by the pioneering work of Kaczanov (1958) describe progressive loss of the material integrity due to the propagation and coalescence of microcracks and microvoids. They can be relatively simple, i.e. isotropic (Peerlings et al. 1998, Geers et al. 1998, Jirasek 2004) or more complex, i.e. anistropic (Zhou et al. 2002, Krajcinovic and Fonseka 1981, Kuhl and Ramm 2000). The simplest isotropic damage model describes the degradation of the material due to micro-cracking with the aid of a single scalar damage parameter D growing from 0 (undamaged state) to 1 (completely damaged state). Thus, the stress-strain law is represented by the following relationship:

$$\sigma_{ij} = (1 - D) \, C^e_{ijkl} \varepsilon_{kl}, \tag{1}$$

where σ_{ij} is the stress tensor, C_{ijkl} denotes the linear elastic material stiffness matrix and ε_{kl} is the strain tensor. Thus, the damage variable D acts as an isotropic stiffness reduction factor. It is assumed by Eq. 1 that the Poisson ratio is not affected by damage. The growth of the damage variable D is controlled by a damage threshold parameter κ characterizing the maximum of the equivalent strain measure $\widetilde{\varepsilon}$ (scalar measure) reached during the previous history of the material up to a given time t:

$$\kappa = \max_{\tau \le t} \widetilde{\varepsilon} \, (\tau) \,. \tag{2}$$

During monotonic loading, the parameter κ grows (it coincides with $\widetilde{\varepsilon}$), and during unloading it remains constant (while $\widetilde{\varepsilon}$ decreases). The history variable κ for loading-unloading conditions is defined by the Kuhn-Tucker relations:

$$\overset{\bullet}{\kappa} \ge 0, \quad \widetilde{\varepsilon} - \kappa \le 0, \quad \overset{\bullet}{\kappa} \left(\widetilde{\varepsilon} - \kappa \right) = 0 \tag{3}$$

and an initial value of κ_o.

To define the equivalent strain measure $\widetilde{\varepsilon}$, a modified von Mises definition in terms of strains was used following de Vree et al. (1995) and Peerlings et al. (1998):

$$\widetilde{\varepsilon} = \frac{k-1}{2k\,(1-2\nu)}I_1 + \frac{1}{2k}\sqrt{\frac{(k-1)^2}{(1-2\nu)^2}I_1^2 + \frac{12k}{(1+\nu)^2}J_2},\qquad(4)$$

where I_1 and J_2 are first invariant of the strain tensor and the second invariant of the deviatoric strain tensor, respectively:

$$I_1 = \varepsilon_{11} + \varepsilon_{22} + \varepsilon_{33}, \quad J_2 = \frac{1}{2}\varepsilon_{ij}\varepsilon_{ij} - \frac{1}{6}I_1^2.\qquad(5)$$

The parameter k in Eq. 4 denotes the ratio between the compressive and tensile strength of the material. A two-dimensional representation of Eq. 4 is given in Fig. 1 for $k = 10$. The curve approximately describes the behaviour of concrete during a biaxial test (in a principal strain space). The shape of the curve is similar in a principal stress space. The stress increment resulting due the change of the damage parameter D is normal to each bound curve of $\widetilde{\varepsilon}$ (Eq. 2). Other definitions of the equivalent strain measure $\widetilde{\varepsilon}$ were used for concrete by Mazars and Pijaudier-Cabot, 1989 (using principal strains separately in tension and compression) and by Jirasek, 2004 (using principal stresses of the Rankine criterion).
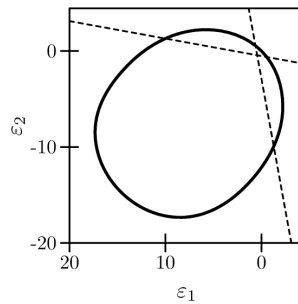

Fig. 1. Equivalent strain definition in principal strain space for plane stress (Peerlings et al. 1998)

To describe the evolution of the damage variable D, an exponential softening law was used to describe the concrete behaviour during uniaxial tension (Peerlings et al. 1998), Fig. 2a:

$$D = 1 - \frac{\kappa_0}{\kappa}\left(1 - \alpha + \alpha e^{-\beta(\kappa-\kappa_0)}\right),\qquad(6)$$

wherein κ_0 is the initial value of the damage threshold parameter κ, and α and β are the material parameters. The damage evolution law determines the shape of the softening curve, i.e. the material brittleness (Fig. 2b). The material softening

starts when the axial strain reaches the initial threshold κ_0 (material hardening is neglected). The parameter β determines the rate of the damage growth (larger value of β causes a faster damage growth). For $\varepsilon \to \infty$ (uniaxial tension), the stress approaches the value of $(1 - \alpha)E\kappa_0$ (Fig. 2b). The shape of the curve of Fig. 2b is quantitatively in accordance with tension uniaxial tests (Hordijk 1991). Due to numerics one assumed an asymptotic character of this curve for large strains. The shape of the load-displacement curve during an uniaxial compression is similar to that in a uniaxial tension of Fig. 2b (linear up to the peak and non-linear in a softening regime). Alternative forms of the damage evolution law were proposed by Geers et al. (1998), Zhou et al. (2002) and Jirasek (2004).
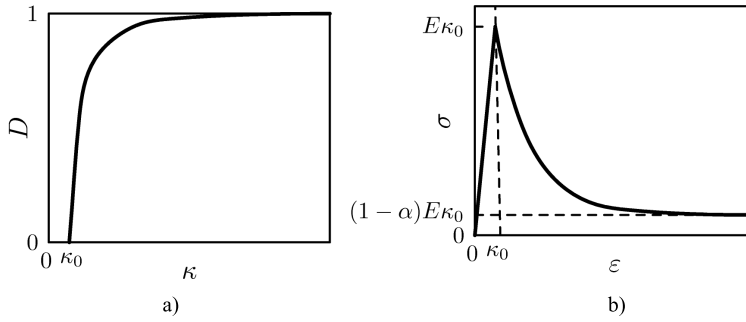

Fig. 2. Damage model: a) damage variable as a function of κ, b) homogeneous stress-strain behaviour during uniaxial tension (E – modulus of elasticity, Peerlings et al. 1998)

3. Non-Local Approach

To preserve the well-posedness of the boundary value problem and to obtain mesh-independent results, a non-local theory was used as a regularisation technique (Bazant 1986, Pijaudier-Cabot and Bazant 1987, Bazant and Lin 1988, Brinkgreve 1994). A full non-local model assumes a relationship between average stresses $\bar{\sigma}_{ij}$ and averaged strains $\bar{\varepsilon}_{ij}$ defined as

$$\bar{\sigma}_{ij}(x_k) = \frac{1}{A} \iiint w\left(x_k'\right) \sigma_{ij}\left(x_k + x_k'\right) dx_1' dx_2' dx_3' \tag{7}$$

and

$$\bar{\varepsilon}_{ij}(x_k) = \frac{1}{A} \iiint w\left(x_k'\right) \varepsilon_{ij}\left(x_k + x_k'\right) dx_1' dx_2' dx_3', \tag{8}$$

where x_k are the global coordinates, x_k' are the local coordinates, w denotes the weighting function and A stands for the weighted volume:

$$A = \iiint w\left(x_k'\right) dx_1' dx_2' dx_3'. \tag{9}$$

For the sake of simplicity, the local coordinates x'_k can be replaced by the distance r measured from each material point to other points of the body:

$$\overline{\sigma}_{ij}(x_k) = \frac{1}{A}\int w(r)\,\sigma_{ij}(x_k + r)\,dV \tag{10}$$

and

$$\overline{\varepsilon}_{ij}(x_k) = \frac{1}{A}\int w(r)\,\varepsilon_{ij}(x_k + r)\,dV. \tag{11}$$

In general, it is required that the weighting function should not alter a uniform field which means that it must satisfy the normalizing condition (Bazant and Jirasek 2002). Therefore, as a weighting function w in Eq. 8, the Gauss distribution function was used:

$$w = \frac{1}{l_c\sqrt{\pi}}e^{-\left(\frac{r}{l_c}\right)^2}, \tag{12}$$

where the parameter l_c is a characteristic length. The averaging in Eq. 12 is restricted to a small representative area around each material point (the influence of points at the distance of $r = 3 \times l_c$ is only of 0.1%, Fig. 3). The characteristic length is related to the micro-structure of the material (e.g. maximum aggregate size and spacing in concrete, pore and grain size in granulates, crystal size in metals). It lies between $3 \times d_a$ and $5 \times d_a$, where d_a is the maximum aggregate size (Bazant and Pijaudier-Cabot 1989). It is usually determined with an inverse identification process of experimental data (Geers et al. 1996, Mahnken and Kuhl 1999). Recently, Le Bellego et al. (2003) presented a calibration method of non-local models containing an internal length on the basis of four size effect bending tests. However, the determination of one representative characteristic length of micro-structure is very complex in concrete since strain localization can include a mixed mode (cracks and shear zones, Bazant and Jirasek 2002), the characteristic length is one-dimensional but is related to the fracture process zone with a certain area or volume (Bazant and Jirasek 2002) and varies (mainly increases) with changing fracture zone size (on the basis of acoustic emission measurements, Pijaudier-Cabot et al. 2004a, b).

Other functions can also be used for the function w (di Prisco et al. 2002, Bazant and Jirasek 2002, Ozbolt 1995, Akkermann 2000, Jirasek 2004); e.g. the polynomial bell-shaped function reads:

$$w = \left(1 - \frac{r^2}{R^2}\right)^2, \tag{13}$$

where R (interaction radius) is a parameter related to the characteristic length. It is sufficient to introduce non-locality only to one variable controlling the degradation of the material (the stresses and strains remain local, Bazant and Lin
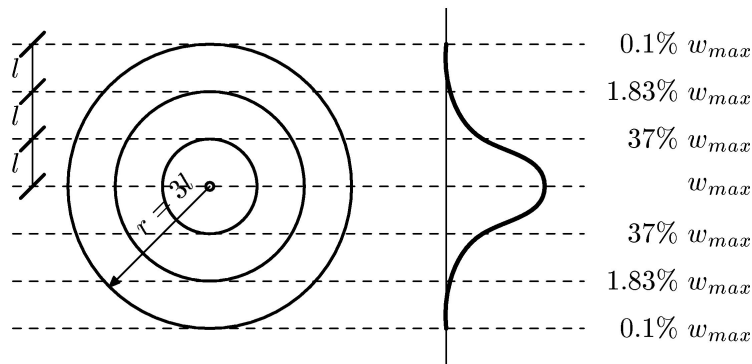
Fig. 3. Region of the influence of a characteristic length l_c and weighting function w

1988, Maier 2002, 2003, Bobinski and Tejchman 2004). To improve the behaviour of a non-local averaging in the vicinity of the boundary of a finite body, Polizzotto et al. (1998) proposed the weight distribution preserving a uniform field and symmetry:

$$w' = w(r) + \left[1 - \int_V w(\xi)d\xi \right] \delta(r),$$ (14)

where δ denotes the Dirac distribution. This function is thus corrected by a suitable multiple of the local value to compensate for boundary effects. The FE-results by Jirasek et al. (2004), show that the type of a non-local averaging near boundaries influences the peak of the load-displacement curve; the averaging with a symmetric local correction by Eq. 14 results in lower resistance.

The FE-analyses show that the finite element size should be small enough compared to l_c (at least one third of l_c) (Le Bellego et al. 2003).

In the FE-calculations, the equivalent strain measure $\widetilde{\varepsilon}$ in Eq. 4 was replaced by its non-local definition $\bar{\varepsilon}$ following Eq. 11:

$$\bar{\varepsilon}(x_k) = \frac{1}{A} \int w(r)\widetilde{\varepsilon}(x_k + r)\,dV.$$ (15)

4. FE-Data

The non-local model was implemented in the commercial finite element code Abaqus (2001) for efficient computations. During calculations, two identical overlapping meshes were used. The first mesh allowed to gather the information about coordinates of integration points in the entire specimen, area of all finite elements and total strain rates in each element. The elements in this mesh were defined by the user in the UEL procedure. They did not influence the results of stresses in

the specimen body since they had no stiffness. The information stored was needed to calculate non-local variables with the aid of the second mesh which included standard elements from the Abaqus library. The constitutive law was defined by the UMAT procedure. During odd iterations, the information was gathered in the elements of the first mesh. During even iterations, the stresses in the elements of the second mesh (including standard elements) were determined, taking into account non-local variables and a non-linear finite element equation was solved. Between odd and even iterations, the same element configuration was imposed.

For the solution of the non-linear equation of motion governing the response of a system of finite elements, a modified Newton-Raphson scheme was used. The calculations were performed with a symmetric elastic global stiffness matrix. The calculations with a full Newton-Raphson method resulted in worst convergency in the softening regime. The following convergence criteria were assumed:

$$r_{\max} \leq 0.01\widetilde{q} \quad \text{and} \quad c_{\max} \leq 0.01\Delta u_{\max}, \tag{16}$$

where $r_{\max}$ – the largest residual out-of-balance force, $\widetilde{q}$ – spatial averaged force over the entire body, $c_{\max}$ – the largest correction of the displacement and $\Delta u_{\max}$ – the largest change of the displacement in the increment. The procedure yielded a sufficiently accurate and fast convergence. The magnitude of the maximum out-of-balance force at the end of each calculation step was smaller than 1% of the calculated total vertical force on the specimen. The calculations with the smaller tolerances in Eq. 16 did not influence the FE-results. The integration was performed in one sample point of each element (centroid).

The calculations were carried out using a large-displacement analysis available in the Abaqus finite element code. In this method, the actual configuration of the body was taken into account. The Cauchy stress was taken as the stress measure. The conjugate strain rate was the rate of deformation. The rotation of the stress and strain tensor was calculated with the Hughes-Winget method (Hughes and Winget 1980). The non-local averaging was performed in the current configuration.

5. Numerical Results

5.1. Uniaxial Tension

The problem of a double notched specimen under uniaxial tension was experimentally investigated by Hordijk (1991) and numerically analysed by Peerlings et al. (1998) and Pamin (2004) using a second-gradient damage continuum model. The geometry of the concrete specimen (width $b = 60$ mm, height $h = 125$ mm, thickness in the out-of-plane direction $t = 50$ mm) and boundary conditions are presented in Fig. 4. Two symmetric notches 5×5 mm^2 were located at the mid-point of both sides of the specimen. All nodes along the bottom were fixed

in the vertical direction. The top and bottom were smooth. To preserve the stability of the specimen, the node in the middle of the bottom was fixed in the horizontal direction. The non-local parameters along all boundaries of the specimen were calculated without modifications. The vertical tensile deformation was imposed by enforcing the vertical dispacement Δv of all nodes along the upper edge (Fig. 4). The modulus of elasticity was equal to $E = 18$ GPa and the Poisson's ratio was $\upsilon = 0.2$ (Peerlings et al. 1998). The following parameters of the damage model were chosen (Eqs. 4 and 6): $\kappa_0 = 2.1 \times 10^{-4}$, $\alpha = 0.96$, $\beta = 500$ and $k = 10$. The characteristic length l_c was assumed to be 5 mm (Eq. 9). Three different FE-meshes were used: coarse (1192 triangular elements), medium (1912 triangular elements) and fine (4168 triangular elements), Fig. 5. When calculating non-local quantities close to the notches, the so-called "shading effect" was considered (Pamin 2004), i.e. the averaging procedure considered the notches as an internal barrier that was shading the non-local interaction.
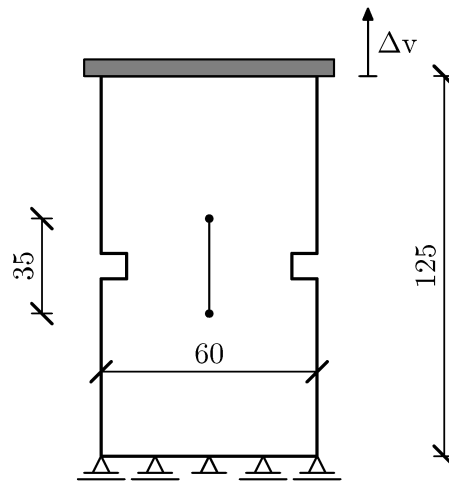

Fig. 4. Geometry and boundary conditions of a specimen with a notch under uniaxial tension (dimensions are given in mm)

The calculated contours of the damage parameter κ in the specimen are shown in Fig. 6 for a residual state. The results are mesh-independent, since the width of the damage region in the mid-region of the specimen is always the same. The width of the localization zone was approximately 22 mm ($4.4 \times l_c$).

Fig. 7 presents the nominal stress–elongation tensile curves for all meshes as compared to the experimental curve (Hordijk 1991). The elongation δ in Fig. 7 denotes the elongation of the specimen above and below both notches at the height of 35 mm, Fig. 5. It was measured experimentally by 4 pairs of extensometers with a gauge length of 35 mm. The vertical normal stress was calculated by
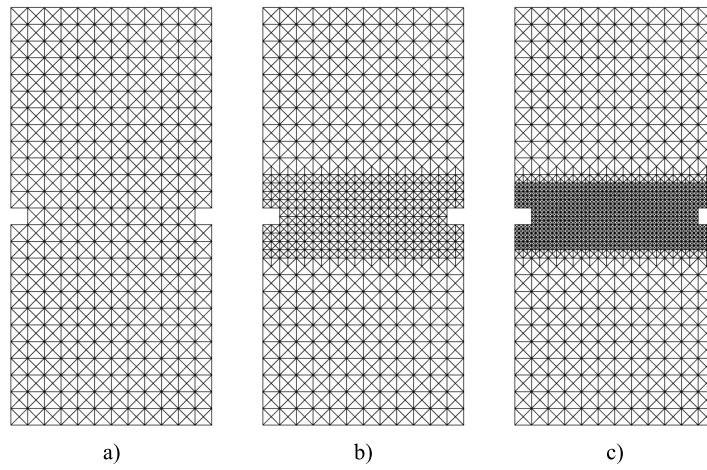
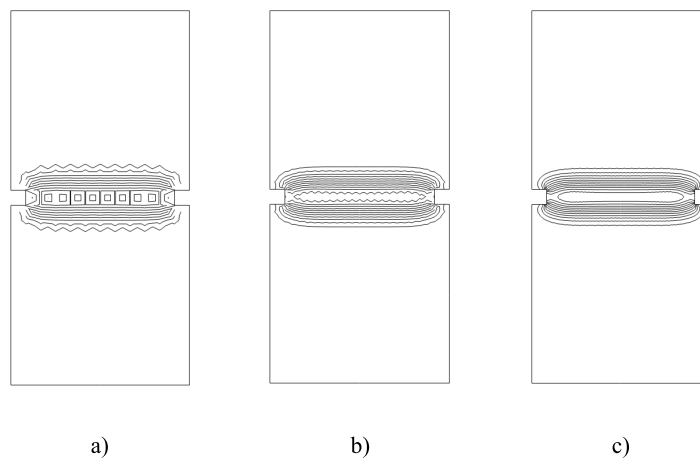**Fig. 5.** FE-meshes used for calculations of uniaxial tension: a) coarse, b) medium, c) fine

Fig. 6. Calculated contours of the damage parameter κ in a specimen under uniaxial tension for:
a) coarse, b) medium and c) fine mesh

dividing the calculated resultant vertical force along the upper edge by the specimen cross-section of 50×50 mm^2. The calculated load-displacement curves of Fig. 8 practically coincide for the different meshes. They are also in a satisfactory conformity with the experimental curve of Fig. 7, although a deviation between the theory and the experiment, in particular before the peak (due to the lack of hardening) and after the peak, takes place.
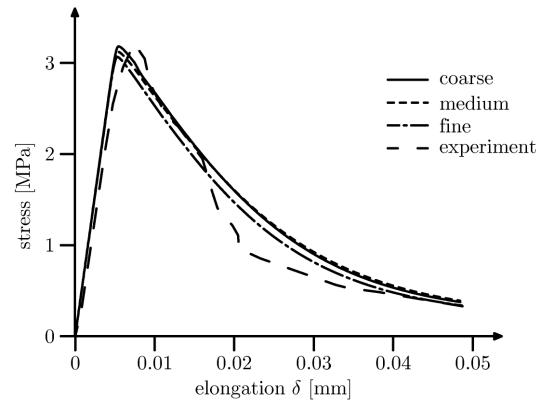

Fig. 7. Calculated stress–elongation diagrams for a specimen under uniaxial tension with different FE-meshes compared to the experimental diagram (Hordijk 1991)
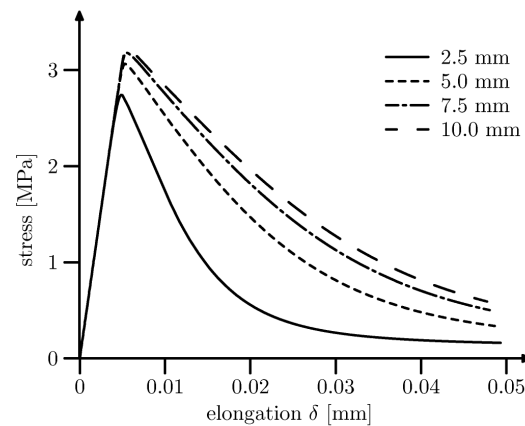

Fig. 8. Calculated stress–elongation diagrams using different characteristic lengths l_c for a specimen under uniaxial tension

In addition, the influence of the characteristic length l_c of micro-structure on the specimen behaviour was investigated. The FE-calculations were performed with l_c in the range of from 2.5 mm up to 10.0 mm. The obtained load-displacement curves are presented in Fig. 8. The larger the characteristic

length l_c, the higher the maximum tensile stress. The inclination of all curves to the horizontal after the peak becomes smaller with increasing l_c (the material becomes more ductile). The width of the localized zone was 12 mm ($4.8 \times l_c$ for $l_c = 2.5$ mm), 22 mm ($4.4 \times l_c$ for $l_c = 5$ mm), 34 mm ($4.5 \times l_c$ for $l_c = 7.5$ mm) and 44 mm ($4.4 \times l_c$ for $l_c = 10$ mm), Fig. 9.
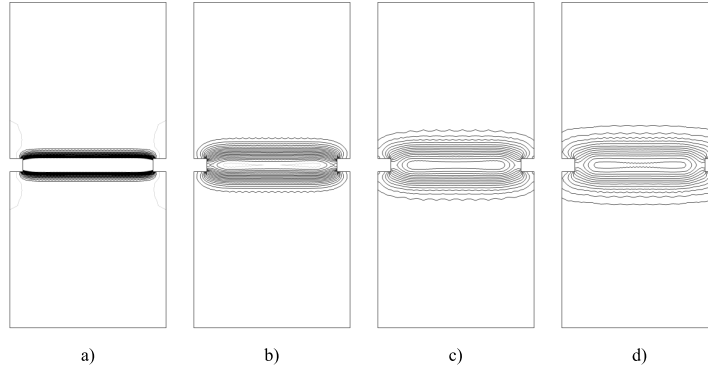

a)   b)   c)   d)

Fig. 9. Calculated contours of the damage parameter κ in a specimen under uniaxial tension for fine mesh: a) $l_c = 2.5$ mm, b) $l_c = 5$ mm, c) $l_c = 7.5$ mm, d) $l_c = 10$ mm

The load-displacements curves are in a good accordance with the FE-results by Peerlings et al. (1998) and Pamin (2004).

5.2. Three-Point Bending

The problem of a notched beam under three-point bending was experimentally studied by Kormeling and Reinhardt (1983) and numerically simulated by Jirasek (2004) using a non-local damage continuum model. The geometry of the beam with a depth of $t = 100$ mm is shown in Fig. 10 (length $l = 450$ mm, height $h = 100$ mm). The deformation was obtained by imposing the vertical displacement Δv to the top at the mid-span of the beam. The elastic properties were: $E = 20$ GPa and $v = 0.2$. The following damage parameters were chosen: $\kappa_0 = 1.2 \times 10^{-4}$, $\alpha = 0.96$, $\beta = 200$, and $k = 10$ (Eqs. 1–5). The characteristic length was $l_c = 5$ mm. The calculations were carried out also with $\beta = 500$. A coarse (2120 elements) medium (2300 elements) and fine (4380 elements) mesh was used.

The calculated contours of the damage parameter κ at residual state are shown in Fig. 11. The results are mesh-independent. The width of the localization zone is approximately equal to 23 mm ($4.5 \times l_c$). In turn, Fig. 12 presents the calculated load–displacement curves for different meshes which are almost indentical and match well with two experimental curves (Kormeling and Reinhardt 1983) – they lie between them – for the parameter $\beta = 200$. The effect of β on the load-displacement diagram is strong. The larger the β, the smaller the beam strength. The results with different characteristic lengths l_c ($l_c = 2$–10
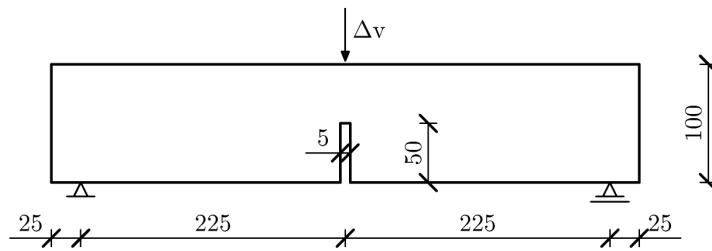
Fig. 10. Geometry and boundary conditions of the beam under three-point bending
(dimensions are given in mm)

mm), indicate that the beam strength increases with increasing l_c (Fig. 13). Thus, a pronounced size effect caused by the ratio l_c/L (L – specimen size) occurs. With increasing characteristic length, the behaviour of the material after the peak becomes more ductile. The Fe-results are very similar to the FE-results by Jirasek (2004).
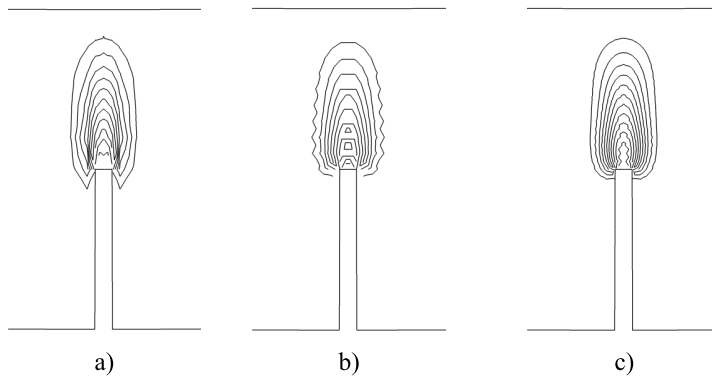

a)   b)   c)

Fig. 11. Calculated contours of the damage parameter κ near the notch of the beam under three-point bending for: a) coarse, b) medium and c) fine mesh

5.3. Four-Point Bending

The problem of a notched beam under four-point bending was experimentally investigated by Hordijk (1991) and numerically simulated by both Pamin (2004) with second-gradient plasticity and Simone et al. (2002) with a second-gradient damage model. The geometry of the specimen is given in Fig. 14 (length $l = 450$ mm, height $h = 100$ mm). The beam had a 5×10 mm^2 notch at the mid-span. The thickness of the beam in out-of-plane direction was $t = 50$ mm. The deformation was induced by imposing a vertical displacement Δv in two nodes at the top in the central part of the beam. The modulus of elasticity was $E = 40$ GPa and the Poisson's ratio $v = 0.2$. The remaining material parameters were: $\kappa_0 = 0.75 \times 10^{-4}$,
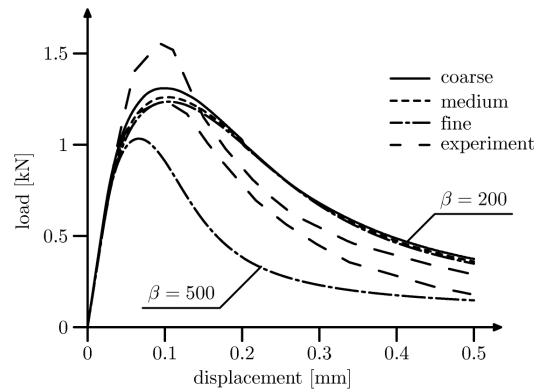
Fig. 12. Calculated load–displacement diagrams for a beam under three-point bending with different FE-meshes compared to the experimental curves (Kormeling and Reinhardt 1983)
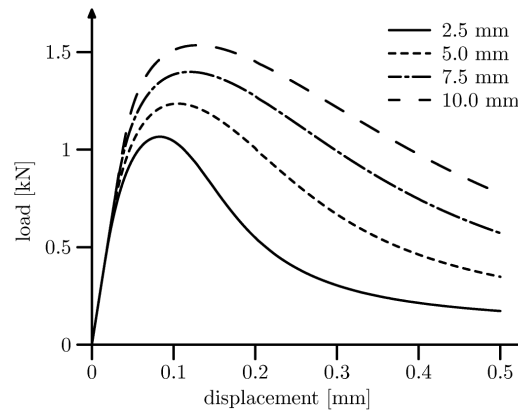

Fig. 13. Calculated load–displacement diagrams for different characteristic lengths l_c (beam under three-point bending)

$\alpha = 0.92$, $\beta = 200$, $k = 10$ and $l_c = 5$ mm. The FE-analyses were carried out with a coarse (2152 elements) medium (2332 elements) and fine (4508 elements) mesh.

The calculated contours of the damage parameter κ are shown in Fig. 15. The obtained results do not depend on the mesh size. The width of the localization zone is approximately equal to 26 mm ($5.2 \times l_c$). Fig. 16 depicts the load–displacment curves for various FE-meshes which are almost indentical. They are also close to the experimental curve (Hordijk 1991). In addition, the influence of the characteristic length in the range of $l_c = 2.5$–10.0 mm was analyzed (Fig. 17). The results of Fig. 17 show that the effect of the characteristic length on the load-displacement diagrams is pronounced.

The load-displacement diagrams are quantitatively close to the solutions given by Simone et al. (2002) and Pamin (2004).
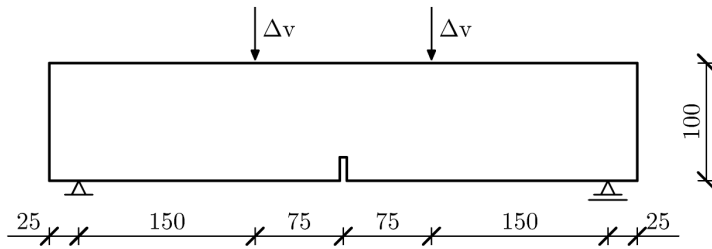
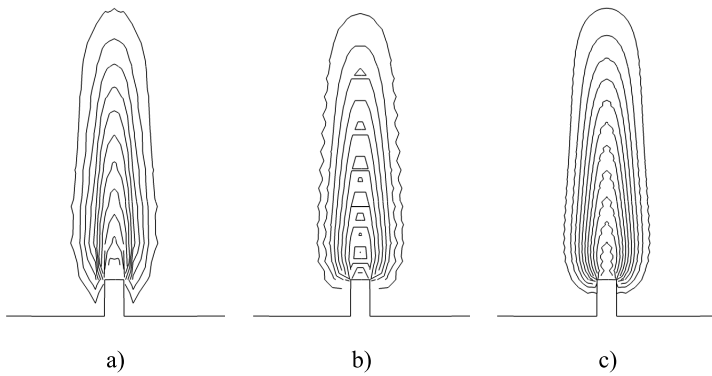**Fig. 14.** Geometry and boundary conditions of the beam under four-point bending (dimensions are given in mm)

a)   b)   c)

Fig. 15. Calculated contours of the damage parameter κ near the notch for a beam under four-point bending for different FE-meshes: a) coarse, b) medium and c) fine mesh
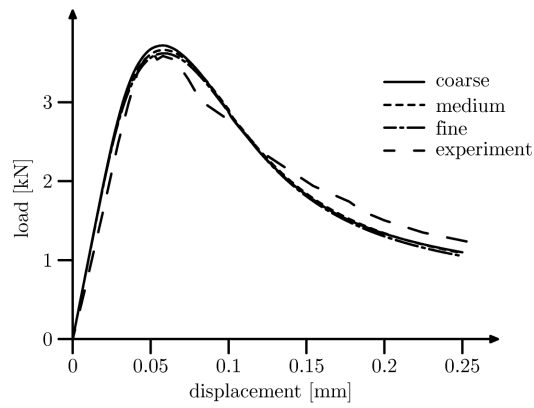

Fig. 16. Calculated load displacement diagrams for a beam under four-point bending for different meshes compared to the experiment (Hordijk 1991)
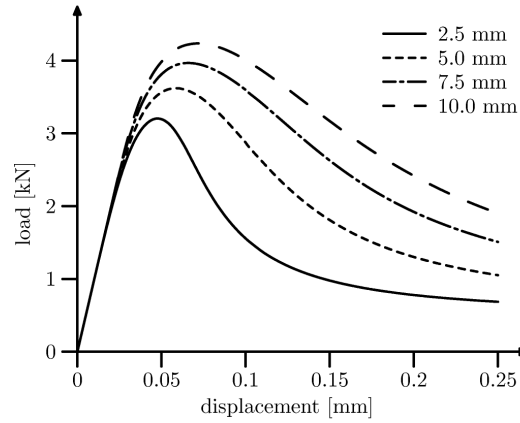
Fig. 17. Calculated load–displacement diagrams for different characteristic lengths l_c (beam under four-point bending)
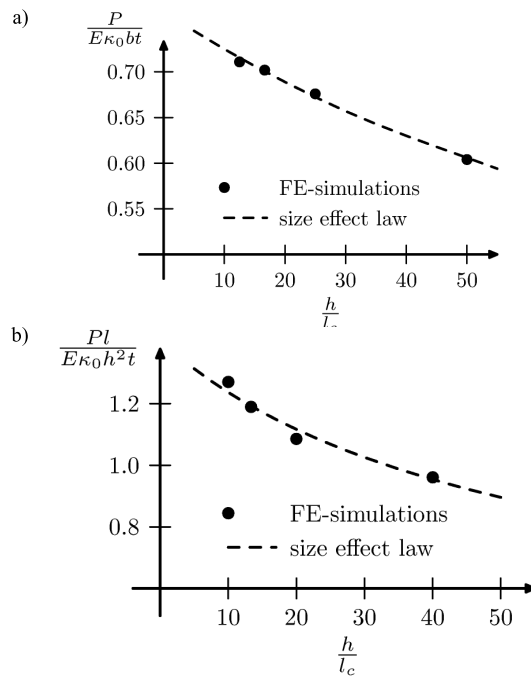

Fig. 18. Relationship between the calculated normalized strength $P/E\kappa_{0t}bt$ (uniaxial tension) (a) and $Pl/E\kappa_0h^2t$ (four-point bending) (b) and ratio h/l_c compared to the size effect law (Bazant 1984)

Fig. 18 shows the calculated size effect expressed by the normalized strength $P/E\kappa_0 bt$ (uniaxial tension) and $Pl/E\kappa_0 h^2 t$ (four-point bending) against the ratio h/l_c. The normalized strength decreases almost linearly with the size ratio h/l_c in the considered range. The relationship can be approximated by the Bazant's size effect formula (Bazant 1984), wherein two required parameters were calculated using a linear regression.

6. Conclusions

- The FE-calculations show that a non-local damage continuum model in spite of its great simplicity is capable of modelling strain localization in quasi-brittle materials during uniaxial tension and bending. The obtained FE-results do not suffer from the mesh sensitivity. Satisfactory agreement between numerical simulations and experiments was achieved.

- The greater the ratio between the characteristic length of micro-structure and the specimen size, the higher both the bearing capacity and ductility of the specimen.

- The thickness of the localized zones increases with increasing characteristic length of micro-structure. It is about 5 times the characteristic length.

- The size effect is more pronounced during beam bending than during uniaxial tension.

- The greater the value of the parameter β, the faster the damage growth. For uniaxial tension, the most realistic value of β is 500. In turn, for bending, the most realistic value of β turns out to be 200.

- The calculated size effect decreases almost linearly with decreasing ratio between the specimen size and characteristic length in the considered range. It is in agreement with the size effect formula by Bazant.

- A non-local model can be implemented in commercial finite element codes.

- The numerical calculations of strain localization in concrete with a non-local continuum model will be continued. To include plastic deformation and hardening, the damage model will be combined with an elasto-plastic model (Bobinski and Tejchman 2004) according to the proposal by Pamin and de Borst (1999). Afterwards, a damage model will be enriched by anisotropy (Zhou 2002). The FE-calculations will also be performed with reinforced concrete elements by taking into account the slip bond between concrete and reinforcement (Pamin and de Borst 1998). The results will be checked again by experiments and simulations with a discrete lattice model (Bobinski et al. 2005).

Acknowledgments

References

Abaqus 6.1 Manuals (2001), Hibbitt, Karlsson and Sorensen Inc.

Akkermann J. (2000), Rotationsverhalten von Stahlbeton-Rahmenecken, *Dissertation*, Universität Fridericiana zu Karlsruhe, Karlsruhe.

Askes H., Sluys L. J. (2003), A classification of higher-order strain gradient models in damage mechanics, *Arch. Appl. Mech.*, 53 (5–6), 448–465.

Bazant Z. P. (1984), Size effect in blunt fracture: Concrete, rock, metal, *J. Engng. Mech.*, 111, 518–535.

Bazant Z. P. (1986), Mechanics of distributed cracking, *Appl. Mech. Rev.*, 26, 675–705.

Bazant Z. P., Cedolin L. (1979), Blunt crackband propagation in finite rlement analysis, *J. Engng. Mech. Div. ASCE*, 105 (2), 297–315.

Bazant Z. P., Lin F. (1988), Non-local yield limit degradation, *Int. J. Num. Meth. Engng*, 35, 1805–1823.

Bazant Z., Pijaudier-Cabot G. (1989), Measurement of the characteristic length of nonlocal models, *J. Engng. Mech. ASCE*, 115, 755–767.

Bazant Z., Ozbolt J. (1990), Non-Local microplane model for fracture, damage and size effect in structures, *J. Engng. Mech. ASCE*, 116, 2485–2505.

Bazant Z. P., Jirasek M. (2002), Nonlocal integral formulations of plasticity and damage: Survey of progress, *J. Engng. Mech.*, 128, 11, 1119–1149.

Bobinski J., Tejchman J. (2004), Numerical simulations of localization of deformation in quasi-brittle materials within non-local softening plasticity, *Computers and Concrete,* 4, 433–455.

Bobinski J., Kozicki J., Tejchman J. (2005), Modelling of localization of deformation in quasi-brittle materials with a continuum and discrete model, *Proc. Int. Conference on Powders and Grains,* 18–22.07.2005, Stuttgart, Germany, 1441–1445 .

de Borst R. (1986), Non-Linear Analysis of Frictional Materials, *PhD Thesis*, Delft University of Technology.

de Borst R., Pamin J., Geers M. (1999), On coupled gradient-dependent plasticity and damage theories with a view to localization analysis, *Eur. J. Mech. A/Solids*, 18, 6, 939–962.

Brinkgreve R. (1994), Geomaterial Models and Numerical Analysis of Softening, *Dissertation*, Delft University of Technology.

Chen E. P. (1999), Non-local effects on dynamic damage accumulation in brittle solids, *I. J. Num. Anal. Meth. Geomech.*, 23, 1–21.

Chen J., Yuan H., Kalkhof D. (2001), A nonlocal damage model for elastoplastic materials based on gradient plasticity theory, *Report No. 01–13*, Paul Scherrer Institut, 1–130.

Donze F. V., Magnier S. A., Daudeville L., Mariotti C., Davenne L. (1999), Numerical study of compressive behaviour of concrete at high strain rates, *J. Engineering Mechanics*, 1154–1163.

Dragon A., Mróz Z. (1979), A Continuum model for plastic-brittle behaviour of rock and concrete, *Int. J. Eng. Science*, 17, 121–137.

Ehlers W., Graf T. (2003), Adaptive Computation of Localization Phenomena in Geotechnical Applications, [in:] *Bifurcations and Instabilities in Geomechanics* (eds. J. Labuz and A. Drescher), Swets and Zeitlinger, 247–262.

Geers M., Peijs, T., Brekelmans W., de Borst R. (1996), Experimental monitoring of strain localization and failure behaviour of composite materials, *Compos. Sci. Technol.*, 56, 1283–1290.

Geers M., de Borst R., Brekelmans W., Peerlings R. (1998), Strain-based transient-gradient damage model for failure analyses, *Comparative Methods in Applied Mechanics and Engineering*, 160, 1–2, 133–154.

Herrmann H. J., Hansen A., Roux S. (1989), Fracture of disordered elastic lattices in two dimensions, *Physical Rev. B*, 39, 637–647.

Hilleborg A. (1989), The theoretical basis of a method to determine the fracture energy of concrete, *Materials and Structures*, 18, 291–296.

Hordijk D. A. (1991), *Local Approach to Fatigue of Concrete*, Ph. D. dissertation, Delft University of Technology.

Hughes T. J. R., Winget J. (1980), Finite rotation effects in numerical integration of rate constitutive equations arising in large deformation analysis, *Int. J. for Numerical Methods in Engineering*, 15, 1862–1867.

Ibrahimbegovic A., Markovic D., Gatuingt F. (2003), Constitutive model of coupled damage-plasticity and its finite element implementatation, *Eur. J. Finite Elem.*, 12 (4), 381–405.

Jirasek M. (1999), Comments on Microplane Theory, [in:] *Mechanics of Quasi-Brittle Materials and Structures* (eds. G. Pijaudier-Cabot, Z. Bittnar and B. Gerard), Hermes Science Publications, 55–77.

Jirasek M. (2004), Non-Local Damage Mechanics with Application to Concrete, [in:] *Failure, Degradation and Instabilities in Geomaterials* (eds. I. Vardoulakis and P. Mira), Lavoisier, 683–709.

Jirasek M., Rolshoven S. (2003), Comparison of integral-type nonlocal plasticity models for strain-softening materials, *Int. J. Engineering Science*, 41, 1553–1602.

Jirasek M., Rolshoven, S., Grassl P. (2004), Size effect on fracture energy induced by non-locality, *Int. J. for Numerical and Analytical Methods in Geomechanics*, 28, 653–670.

Kaczanov L. M. (1958), Time of the rupture process under creep conditions, *Isv. Akad. Nauk SSSR, Otd. Tèkh. Nauk*, 8, 26–31.

Klisinski M., Mróz Z. (1988), *Description of Unelastic Deformations and Damage for Concrete* (in Polish), *Monography*, 193, Technical University of Poznań.

Kormeling H. A., Reinhardt H. W. (1983), Determination of the Fracture Energy of Normal Concrete and Epoxy Modified Concrete, *Report 5-83-18*, Delft University of Technology.

Krajcinovic D., Fonseka G. U. (1981), The continuous damage theory of brittle materials, *J. Applied Mechanics ASME*, 48, 809–824.

Kuhl E., Ramm E. (2000), Simulation of strain localization with gradient enhanced damage models, *Computational Material Sciences*, 16, 176–185.

Lade P. V., Jakobsen K. P. (2002), Incrementalization of a single hardening constitutive model for frictional materials, *Int. J. Numer. Anal. Methods in Geomech.*, 26, 647–659.

Le Bellego C., Dube J. F., Pijaudier-Cabot G., Gerard B. (2003), Calibration of nonlocal damage model from size effect tests, *E. J. Mechanics A/Solids*, 22, 33–46.

Lemaitre J. (1985), Coupled elasto-plasticity and damage constitutive equations, *Computer Methods Appl. Mech. Eng.*, 51, 31–49.

Loret B., Prevost J. H. (1990), Dynamic strain localization in elasto-visco-plastic solids, Part 1. General formulation and one-dimensional examples, *Comp. Appl. Mech. Eng.*, 83, 247–273.

Mahnken R., Kuhl E. (1999), Parameter identification of gradient enhanced damage models, *Eur. J. Mech. A/Solids*, 18, 819–835.

Maier T. (2002), Numerische Modellierung der Entfestigung im Rahmen der Hypoplastizität, *PhD Thesis*, University of Dortmund.

Maier T. (2003), Nonlocal modelling of softening in hypoplasticity, *Comput. Geotech.*, 30 (7), 599–610.

Marcher T., Vermeer P. A. (2001), Macro-Modelling of Softening in Non-Cohesive Soils, [in:] *Continuous and Discontinuous Modelling of Cohesive-Frictional Materials*, (eds. P. A. Vermeer et al.), Springer-Verlag, 89–110.

Mazars J., Pijaudier-Cabot G. (1989), Continuum damage theory – applications to concrete, *J. Engng. Mech.*, 115, 345–365.

Meftah F., Reynouard J. M. (1998), A multilayered mixed beam element on gradient plasticity for the analysis of localized failure modes, *Mechanics of Cohesive-Frictional Materials*, 3, 305–322.

Menetrey Ph., Willam K. J. (1995), Triaxial failure criterion for concrete and its generalization, *ACI Structural Journal*, 311–318.

Mühlhaus H.-B. (1986), Scherfugenanalyse bei Granularen Material im Rahmen der Cosserat-Theorie, *Ingen. Archiv*, 56, 389–399.

Mühlhaus H.-B., Aifantis E. C. (1991), A variational principle for gradient plasticity, *Int. J. Solids Structures*, 28, 845–858.

Neddleman A. (1988), Material rate dependence and mesh sensitivity in localization problems, *Comp. Meths. Appl. Mech. Eng.*, 67, 69–85.

Ozbolt J. (1995), Maßstabseffekt und Duktulität von Beton- und Stahlbetonkonstruktionen, *Habilitation,* Universität Stuttgart.

Pamin J. (2004), Gradient-Enchanced Continuum Models: Formulation, Discretization and Applications, *Habilitation,* Cracow University of Technology, Cracow.

Pamin J., de Borst R. (1998), Simulation of crack spacing using a reinforced concrete model with an internal length parameter, *Arch. App. Mech.*, 68 (9), 613–625.

Pamin J., de Borst R. (1999), Stiffness degradation in fradient-dependent coupled damage-plasticity, *Arch. Mech.*, 51, 3–4, 419–446.

Peerlings R. H. J., de Borst R., Brekelmans W. A. M., Geers M. G. D. (1998), Gradient enhanced damage modelling of concrete fracture, *Mech. Cohes.-Friction. Mater.*, 3, 323–342.

Pietruszczak S., Jiang J., Mirza F. A. (1988), An elastoplastic constitutve model for concrete, *Int. J. Solids Structures*, 24 (7), 705–722.

Pijaudier-Cabot G., Bazant Z. P. (1987), Nonlocal damage theory, *ASCE J. Eng. Mech.*, 113, 1512–1533.

Pijaudier-Cabot G., Haidar K., Loukili A., Omar M. (2004a), Ageing and Durability of Concrete Structures, [in:] *Degradation and Instabilities in Geomaterials* (eds. F. Darve and I. Vardoulakis), Springer Verlag.

Pijaudier-Cabot G., Haidar K., Dube J. F. (2004b), Non-local damage model with evolving internal length, *Int. J. Num. and Anal. Meths. in Geomech.*, 28, 633–652.

Place D., Mora P. (2001), A Random Lattice Solid Model for Simulation of Fault Zone Dynamics and Fracture Processes, [in:] *Bifurcation and Localisation Theory in Geomechanics* (ed. H.-B. Mühlhaus et al.), A. A. Balkema, Rotterdam/Brookfield, 321–333.

Polizzotto C., Borino G., Fuschi P. (1998), A thermodynamic consistent formulation of nonlocal and gradient plasticity, *Mech. Res. Commun.*, 25, 75–82.

di Prisco M., Mazars J. (1996), Crush-crack – a non-local damage model for concrete, *Mechanics of Cohesive-Frictional Materials*, 1, 321–347.

di Prisco C., Imposimato S., Aifantis E. C. (2002), A visco-plastic constitutive model for granular soils modified according to non-local and gradient approaches, *Int. J. Numer. Anal. Meth. Geomech.*, 26, 121–138.

Ragueneau F., Borderie Ch., Mazars J. (2000), Damage model for concrete-Like materials coupling cracking and friction, *Int. J. Num. Anal. Meth. Geomech.*, 5, 607–625.

Regueiro R. A., Borja R. I. (2001), Plane strain finite element analysis of pressure sensitive plasticity with strong discontinuity, *Int. J. Solids and Structures*, 38, 21, 3647–3672.

Sakaguchi H., Mühlhaus H. B. (1997), Mesh Free Modelling of Failure and Localisation in Brittle Materials, [in:] *Deformation and Progressive Failure in Geomechanics* (eds. A. Asaoka, T. Adachi and F. Oka), 15–21.

Simone A., Wells G. N., Sluys L. J. (2002), Discontinuous modelling of crack propagation in a gradient enhanced continuum, *Proc. of the fifth World Congress on Computational Mechanics WCCM V,* Vienna, CDROM.

Simone A., Sluys L. (2004), Continous-Discontinous Modeling of Mode-I and Mode-II Failure, [in:] *Modelling of Cohesive-Frictional Materials* (eds. P.A. Vermeer, W. Ehlers, H. J. Herrmann and E. Ramm), Balkema, 323–337.

Sluys L. J. (1992), Wave Propagation, Localization and Dispersion in Softening Solids, *Dissertation*, Delft University of Technology.

Sluys L. J., de Borst R. (1994), Dispersive Properties of Gradient and Rate-Dependent Media, *Mech. Mater.*, 183, 131–149.

Strömberg L., Ristinmaa M. (1996), FE-Formulation of monlocal plasticity theory, *Comput. Methods Appl. Mech. Engng.*, 136, 127–144.

Tejchman J. (2004), Influence of a characteristic length on shear zone formation in hypoplasticity with different enhancements, *Computers and Geotechnics*, 31, 8, 595–611.

Tejchman J., Wu W. (1993), Numerical study on patterning of shear bands in a cosserat continuum, *Acta Mechanica*, 99, 61–74.

Tejchman J., Herle I., Wehr J. (1999), FE-Studies on the influence of initial void ratio, pressure level and mean grain diameter on shear localization, *Int. J. for Numerical and Analitycal Methods in Geomechanics*, 23, 2045–2074.

Vermeer P. A., Vogler U., Septanika E. G., Stelzer O. (2004), A Strong Discontinuity Method without Locking, [in:] *Modelling of Cohesive-Frictional Materials* (eds. P. A. Vermeer, W. Ehlers, H. J. Herrmann and E. Ramm), Balkema, 381–394.

Vervuurt A., van Mier J. G. M., Schlangen E. (1994), Lattice Model for Analyzing Steel-Concrete Interactions, [in:] *Comp. Methods and Advances in Geomechanics* (eds. Siriwardane and Zaman), Balkema, Rotterdam, 713–18.

de Vree J. H. P., Brekelmans W. A. M., van Gils M. A. J. (1995), Comparison of nonlocal approaches in continuum damage mechanics, *Comput. Struct.*, 55, 581–588.

Willam K. J., Warnke E. P. (1975), Constitutive model for the triaxial behaviour of concrete, *IABSE Seminar on concrete structures subjected to triaxial stress*, Bergamo, Italy, 1–31.

Zbib H. M., Aifantis C. E. (1989), A gradient dependent flow theory of plasticity: Application to metal and soil instabilities, *Appl. Mech. Reviews*, 42 (11), 295–304.

Zhou W., Zhao J., Liu Y., Yang Q. (2002), Simulation of localization failure with strain-Gradient-Enhanced Damage Mechnics, *Int. J. Numer. Anal. Meth. Geomech.*, 26, 793–813.